J. Fluid Mech. (2006), *vol.* 547, *pp.* 137–148.
doi:10.1017/S002211200500683X Printed in the United Kingdom

The route to self-similarity in turbulent jets and plumes

By GUILLAUME CARAZZO, EDOUARD KAMINSKI AND STEPHEN TAIT

Laboratoire de Dynamique des Systèmes Géologiques, Université Paris 7 – Denis Diderot and Institut de Physique du Globe de Paris, 4 place Jussieu, 75252 Paris cédex 05, France

(Received 7 April 2005 and in revised form 8 July 2005)

The description of entrainment in turbulent free jets is at the heart of physical models of some major flows in environmental science, from volcanic plumes to the dispersal of pollutant wastes. The classical approach relies on the assumption of complete self-similarity in the flows, which allows a simple parameterization of the dynamical variables in terms of constant scaling factors, but this hypothesis remains under debate. We use in this paper an original parameterization of entrainment and an extensive review of published experimental data to interpret the discrepancy between laboratory results in terms of the systematic evolution of the dynamic similarity of the flow as a function of downstream distance from the source. We show that both jets and plumes show a variety of local states of partial self-similarity in accordance with the theoretical analysis of George (1989), but that their global evolution tends to complete self-similarity via a universal route. Plumes reach this asymptotic regime faster than jets which suggests that buoyancy plays a role in more efficiently exciting large-scale modes of turbulence.

1. Introduction

Turbulent jets are encountered in diverse natural flows, ranging over orders of magnitude in size. Important examples linked to human or industrial activity are smoke plumes from chimneys or oil fires, effluent from submerged pollution outlets, or even the extreme case of a nuclear accident, while naturally occurring flows include activity of seafloor hydrothermal vents, convection in clouds or, most energetic of all, stratospheric plumes due to explosive volcanic eruptions. These flows are canonical examples of turbulent flow, in particular of the process of turbulent entrainment of ambient fluid in a shear layer within the edges of the jet because this largely controls their dynamics.

The classical approach to turbulent entrainment of Morton, Taylor & Turner (1956) based on macroscopic conservation equations for fluxes of mass, momentum and buoyancy, supposes that turbulent jets are self-similar with respect to dimensionless downstream distance from the source. In this hypothesis of 'complete' self-similarity the entrainment rate is a constant fraction of the vertical velocity of the jet which defines an 'entrainment coefficient', α_e. Numerous experimental studies have provided values of the entrainment coefficient in jets and plumes. For a 'top-hat' description of jets (in which the dynamical variables are supposed constant inside the jet at a given distance from the source and zero beyond an effective radius), measured values vary between 0.10 and 0.16 in plumes and from 0.065 to 0.080 in jets (Fischer *et al.* 1979;

Authors	Flow	Fluid	Nozzle	Method	Re	z^*	α_e
Forstall & Gaylord (1955)	J	L	p	w	–	10–20	0.070
Wang & Law (2002)	J	L	p	l	12700	40–80	0.075
Papanicolaou & List (1988)	J	L	c	l	2460–10900	40–50	0.074
Papanicolaou & List (1988)	J	L	c	l	2460–10900	50–80	0.079
Rosensweig *et al.* (1961)	J	G	c	w	26200	15–35	0.076
Panchapakesan & Lumley (1993)	J	G	p	w	11000	90–120	0.095
Ruden (1933)	J	G	c	w	–	15	0.070
Papanicolaou & List (1988)	P	L	c	l	600	22–40	0.130
Papanicolaou & List (1988)	P	L	c	l	600	41–53	0.126
Papanicolaou & List (1988)	P	L	c	l	600	56–85	0.121
Wang & Law (2002)	P	L	c	l	1550–12700	31–55	0.124
Rouse *et al.* (1952)	P	G	c	w	–	75	0.120
George *et al.* (1977)	P	G	c	w	870	8–16	0.159
Shabbir & George (1994)	P	G	c	w	800–1800	10–28	0.154
Nakagome & Hirita (1977)	P	–	–	–	–	11.5	0.170
Schmidt (1941)	P	–	–	–	–	14.5	0.170

TABLE 1. Experimental conditions and measured values of entrainment coefficient, α_e. Flow: J = jet, P = plume; Fluid: L = liquid, G = gas; Nozzle: p = pipe, c = constriction; Method: w = hot-wire probe anemometers; l = laser-Doppler anemometry and laser-induced fluorescence concentration technique; Re: Reynolds number.

Chen & Rodi 1980; Linden 2000; Kaminski, Tait & Carazzo 2005). The systematic difference between the values measured for jets and for plumes undermines the concept of a universal, constant value of α_e, and suggests that genuinely larger values of α_e in plumes than in jets are likely to be due to buoyancy-enhanced turbulence (List 1982; Kaminski *et al.* 2005). Moreover, the origin of the variability in α_e within jets and plumes remains unexplained. Differences between measurement techniques, the nature of fluids and shapes of nozzles are usually suggested to explain such discrepancies.

Table 1 reports the data available in the literature that we have used as a basis for our study organized according to these criteria, and no definitive trend appears. The data appear to demand a framework with a wider explanation. One approach in the literature has been to assume that the entrainment coefficient is indeed a constant, whose value is best extracted globally from data in a given experiment by applying the 'virtual origin' correction. In the Appendix, we show that, although this correction can be significant ($\sim$20% for α_e) in the case of 'lazy' plumes (Hunt & Kaye 2001), it is negligible ($<$1% for α_e) for the 'forced' plumes of the experiments analysed here. A virtual origin correction cannot, for example, explain the differences between the 'plume' entrainment coefficients measured by different authors in table 1. In an attempt to explain this apparent paradox of conflicting measurements, George (1989) suggested that these differences are due not to experimental errors, but to the restrictive manner in which the concept of self-similarity has been applied. According to George's theoretical analysis universal self-similarity is not required by the mathematical structure of the conservation equations but there can exist a multiplicity of self-preserving states determined by initial conditions.

Richards & Pitts (1993) and Mi, Nobes & Nathan (2001) studied experimentally the influence of the initial conditions on the establishment of self-similarity. Mi *et al.* (2001) generated turbulent free jets issuing from two different nozzles and measured the evolution of the scalar field. They found that the asymptotic centreline decay rate of a jet issuing from a smooth contraction nozzle is a function of Reynolds number

whereas for a jet issuing from a long straight pipe there is no such dependence. They interpreted these observations in terms of differences in the turbulence structure and provided support for the analysis of George (1989). On the other hand, Richards & Pitts (1993), who studied the effects of initial conditions on jets by varying the nozzle and the global density ratio, did not find any discrepancy in their experiments. They explained the differences between experimental studies by contamination of the jet by buoyancy and coflow effects and provided support for the hypothesis of universal self-similarity of the jet far from the source. It thus appears that one single 'local' study is not able to solve the problem introduced by George (1989).

Whilst generating some discord, George (1989) also suggested the path to solve the problem: that an analysis of equations involving second-order quantities (i.e. related to Reynolds stresses) might enable identification of additional physical constraints. We propose to follow this idea here using the equation for the flux of mean kinetic energy (Priestley & Ball 1955), and then to reappraise the data from previous studies within the resulting framework to provide a quantitative answer to the problem of self-similarity in jets and plumes.

2. Theoretical framework

A key point in understanding the evolution of self-similarity is to define a coherent framework that provides a hierarchy between the different phenomena in play. Our main aim is a pragmatic one of arriving at a description of self-similarity adequate for quantifying entrainment. Our approach, detailed in a companion paper (Kaminski *et al.* 2005), is based on a 'top-hat' kinetic energy balance and evaluates the consequences for entrainment if the shape of the profiles of velocity, of reduced gravity and of turbulent stress evolve as a function of distance from the source. In that case, instead of being a universal constant, α_e is a function of the shapes of the (Reynolds-averaged) profiles:

$$\alpha_e = \frac{C}{2} + \left(1 - \frac{1}{A}\right) Ri + \frac{R}{2D}\frac{1}{A}\frac{\mathrm{d}A}{\mathrm{d}z^*}, \tag{2.1}$$

where R is the 'top-hat' jet radius, z^* is the ratio z/D with z the distance from the source and D the source diameter, $Ri = g'R/U^2$ is the local Richardson number, with g' the 'top-hat' reduced gravity and U the 'top-hat' velocity, and A and C are integral profiles that depend on velocity, buoyancy and turbulent stress profiles as

$$A = \frac{\displaystyle\int_0^\infty r^* h(r^*, z)\,\mathrm{d}r^* \int_0^\infty r^* f^3(r^*, z)\,\mathrm{d}r^*}{\displaystyle\int_0^\infty r^* f(r^*, z) h(r^*, z)\,\mathrm{d}r^* \int_0^\infty r^* f^2(r^*, z)\,\mathrm{d}r^*}, \tag{2.2}$$

$$C = \frac{\displaystyle\int_0^\infty r^* h(r^*, z)\,\mathrm{d}r^* \left(\int_0^\infty r^* f^2(r^*, z)\,\mathrm{d}r^*\right)^{0.5} \int_0^\infty r^* j(r^*, z)\frac{\partial f}{\partial r^*}\,\mathrm{d}r^*}{\displaystyle\int_0^\infty r^* f(r^*, z) h(r^*, z)\,\mathrm{d}r^* \int_0^\infty r^* f^3(r^*, z)\,\mathrm{d}r^*}, \tag{2.3}$$

where f, h and j are the shape functions for the profiles of velocity, reduced gravity and turbulent shear stress, respectively, and $r^* = r/b_m$ with b_m a radius scale. We calculate A and C from experimental profiles using the method of least-squares

residual based on the following theoretical fits:

$$f(r^*, z) = \exp\left(\sum_{n=2}^{4} a_n \eta^n\right), \tag{2.4}$$

$$h(r^*, z) = \exp\left(\sum_{n=2}^{4} b_n \eta^n\right), \tag{2.5}$$

$$j(r^*, z) = -2c_0\,[\exp(-c_1(\eta - c_2)) - \exp(-c_1(\eta + c_2))], \tag{2.6}$$

where $\eta = r/z$ and a_n, b_n and c_n are fitting parameters reported in table 2. Such equations for velocity and reduced gravity allow the data near the central axis to be accounted for as well as those far from it by adding parameters for curves. As illustrated by the values of the linear regression coefficient given in table 2, these fits explain the data better than the classical Gaussian fit. Nevertheless, when complete experimental data are not available, Gaussian profiles are retained and A and C take the convenient compact forms

$$A = \tfrac{2}{3}(1 + \lambda^2), \tag{2.7}$$

$$C = -6(1 + \lambda^2) \int_0^\infty r^* \exp(-r^{*2}) j(r^*)\, \mathrm{d}r^*, \tag{2.8}$$

where λ is the ratio of the characteristic $(1/e)$ width of the buoyancy profile to that of the velocity profile. C gives the fraction of the total energy flux available for entrainment due to dissipation by turbulent shear stress and A encompasses the influence of the shape of the velocity and reduced gravity profiles on the transfer of gravitational energy to turbulent stress (Kaminski *et al.* 2005). Complete self-similarity implies that the shapes of the profiles do not depend on z^*, requiring constant A and C. In the case of local self-similarity the profiles may evolve as a function of z^*, and A and C can then be used as a proxy to describe quantitatively the evolution of self-similarity.

We have reappraised all the data from laboratory experiments in the literature that allow a calculation of A and C to check if these are constant, if they change erratically or if they show a systematic evolution as a function of z^*. To use equation (2.1) we focused on jets (no buoyancy flux) and plumes (no momentum flux at the source) for which Ri and R/z are analytically known. In practice experiments have been made on buoyant jets with both finite momentum and buoyancy fluxes at the source. Nevertheless, Fischer *et al.* (1979) defined a characteristic length $L_m = M^{3/4}/B^{1/2}$, with M and B the momentum and buoyancy fluxes at the source respectively, that can be used to define 'pure' jets and 'pure' plumes. Pure jets correspond to $z/L_m < 0.5$, where $Ri \approx 0$ and $R/z = 2\alpha_e$, and pure plumes to $z/L_m > 5$ where $Ri = 8\alpha_e/5$ and $R/z = 6\alpha_e/5$.

Values of C are sparse as they require the measurement of the turbulent stress profile. The available data do not show any systematic variation. They can be considered as constant within the experimental error bars and equal to 0.135 ± 0.005 for both plumes and jets. Values of A shown in figure 1, reveal a systematic variation between jets and plumes, from one experiment to another, and as a function of z^*. This trend is not linked to the fluids, technique or source conditions used in the experiments (table 1). This evolution shows that for both jets and plumes $A \neq$ const, and that the description in terms of local self-similarity only is more accurate, as proposed by George (1989).

Authors	a_2	a_3	a_4	R^2_{bf}	R^2_g	b_2	b_3	b_4	R^2_{bf}	R^2_g	c_0	c_1	c_2	A	C
Forstall & Gaylord (1955)	−102.0	–	–	–	–	−84.2	–	–	–	–	–	–	–	1.47	–
Wang & Law (2002)	−89.0	–	–	–	–	−60.1	–	–	–	–	0.061	129.4	0.017	1.65	0.13
Papanicolaou & List (1988)	−92.5	–	–	–	–	−63.0	–	–	–	–	0.015	200	0.09	1.65	0.13
Papanicolaou & List (1988)	−79.7	–	–	–	–	−51.7	–	–	–	–	0.015	200	0.09	1.69	0.13
Rosensweig *et al.* (1961)	−90.9	−101.3	−783.3	0.986	0.964	−81.2	−39.2	97.1	0.993	0.992	–	–	–	1.54	–
Panchapakesan & Lumley (1993)	−3.3	−533.6	972.3	0.979	0.952	−23.8	−146.9	395.1	0.986	0.984	0.021	160	0.06	1.80	0.13
Ruden (1933)	−94.3	–	–	–	–	−54.3	–	–	–	–	–	–	–	1.54	–
Papanicolaou & List (1988)	−90.7	–	–	–	–	−79.4	–	–	–	–	0.015	200	0.09	1.42	0.13
Papanicolaou & List (1988)	−95.5	–	–	–	–	−80.1	–	–	–	–	0.015	200	0.09	1.47	0.13
Papanicolaou & List (1988)	−112.2	–	–	–	–	−93.0	–	–	–	–	0.015	200	0.09	1.49	0.13
Wang & Law (2002)	−147.6	1403.1	−8004.4	0.997	0.990	−84.2	–	–	–	–	0.021	224.4	0.068	1.45	0.14
Rouse *et al.* (1952)	−165.7	669.8	−1358.9	0.926	0.898	−85.9	15.9	369.7	0.974	0.967	–	–	–	1.60	–
George *et al.* (1977)	−87.0	466.7	−1237.9	0.961	0.922	−29.0	−524.9	1987.6	0.982	0.977	–	–	–	1.08	–
Shabbir & George (1994)	−101.8	480.4	−1281.8	0.948	0.936	−73.3	−137.6	541.3	0.975	0.959	0.029	120	0.07	1.17	0.15
Nakagome & Hirita (1977)	−48.2	–	–	–	–	−62.9	–	–	–	–	–	–	–	1.18	–
Schmidt (1941)	−48.2	–	–	–	–	−57.3	–	–	–	–	–	–	–	1.23	–

TABLE 2. Curve-fitting results for velocity (a_n), reduced gravity (b_n) and turbulent shear stress (c_n) profiles and calculated values of A and C. R^2_{bf} and R^2_g give the linear regression coefficient for best-fit profiles and for Gaussian profiles, respectively.

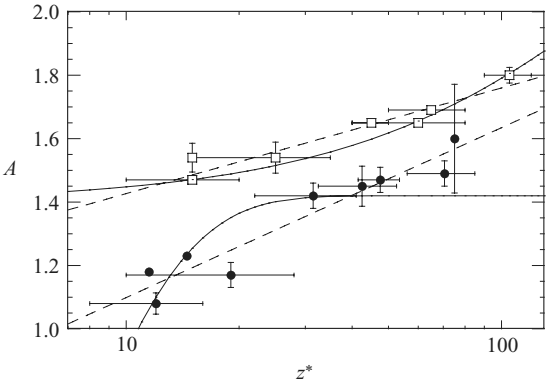

FIGURE 1. Evolution of A as function of z^* in jets (□) and plumes (●). Dashed lines give the best fits and solid lines give the self-consistent fits (see § 3).

3. The route to self-similarity

The evolution of A as a function of z^* visible in figure 1 suggests that although the apparent self-similarity often reported from individual experimental studies can only at best be local, it is possible that taken altogether the experimental data could be interpeted in terms of a universal evolution of self-similarity. To test this, the value of A deduced from the experimental profiles is not the only information we have. In addition, we can use the direct experimental measurement of spreading angle of the velocity profile that, for pure jets and plumes, constitutes a measurement of entrainment constant that can be compared to the theoretical prediction of our parameterization of entrainment (equation (2.1)) as a function of A.

A first reaction to figure 1 might be to propose a simple log-linear best fit to the evolution of A as a function of z^*:

$$A_p = 0.53 + 0.56\log(z^*) \tag{3.1}$$

for plumes and

$$A_j = 1.12 + 0.31\log(z^*) \tag{3.2}$$

for jets, shown as dashed lines. Figure 2 shows however that substituting these best fits for A into (2.1) does not provide good estimates of α_e for both jets and plumes. It also seems unlikely that A goes on increasing as z^* tends to infinity. We therefore search for an empirical description of all the data taken together that optimizes fits to the data for A and for α_e under the constraint that $\mathrm{d}A/\mathrm{d}z^*$ eventually tends to zero for large z^*. We refer to this in figure 1 and subsequent graphs as the self-consistent model. Exponential laws provide the simplest self-consistent fits, namely,

$$A_p = 1.42 - 4.42\exp(-2.188 \times 10^{-1} z^*) \tag{3.3}$$

for plumes and

$$A_j = 2.45 - 1.05\exp(-4.65 \times 10^{-3} z^*) \tag{3.4}$$

for jets. Figure 1 shows that these predict relatively well the evolution of A except perhaps for the value proposed by Rouse *et al.* (1952) ($A = 1.60$ at $z^* = 75$). This however is an older measurement with the largest error bar and the alternative recent value proposed by Wang & Law (2002) ($A = 1.45$ at the same z^*) agrees with the

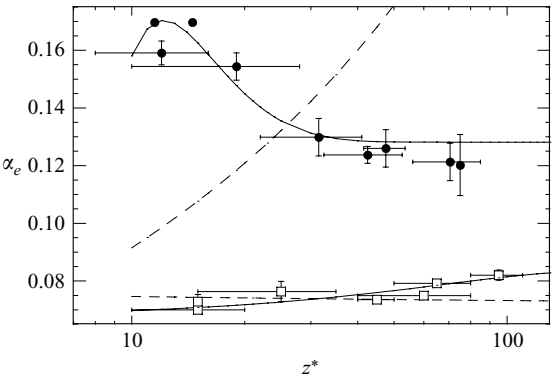

FIGURE 2. Measured evolution of α_e in jets and plumes. The symbols are the same as in figure 1. Dashed lines correspond to predictions with the best fits of A and solid lines give the predictions with the self-consistent fits of A.

self-consistent fit. Figure 2 shows that these exponential laws yield much better estimates of α_e for $z^* > 10$ and account well for the differences between experiments. We chose in our study to exclude the data for z^* lower than 10 for which it is generally agreed that there is a potential core into which mixing has not fully penetrated. We thus conclude that the evolution of entrainment in jets and plumes is determined by the evolution of A. One may note for example the non-monotonic evolution of α_e for plumes at low z^* which corresponds to the dominant influence of the $\mathrm{d}A/\mathrm{d}z^*$ term in (2.1) at lowest z^* whereas at large z^* the flow goes to complete self-similarity and $\mathrm{d}A/\mathrm{d}z^*$ tends to 0. To illustrate the self-consistency of these conclusions, we use our parameterization of entrainment (equation (2.1)) to go back to the rate of change of A as a function of z^*. To do so, one needs the value of C and of the entrainment constant for the different experiments, given in table 1, and to replace Ri and R/z by their expressions for pure jets and pure plumes. Our formula gives for plumes

$$\frac{\mathrm{d}A_p}{\mathrm{d}z^*} = \frac{A_p}{z^*}\left(\frac{8}{3A_p} - 1 - \frac{5C}{6\alpha_e}\right), \tag{3.5}$$

and for jets

$$\frac{\mathrm{d}A_j}{\mathrm{d}z^*} = \frac{A_j}{z^*}\left(1 - \frac{C}{2\alpha_e}\right), \tag{3.6}$$

The rates of change of A estimated from these relationships are shown in figure 3. For plumes, it appears that the rate of change of A decreases as a function of the distance from the source and becomes equal to 0 within experimental errors at approximately $z^* = 50$, which shows that universal self-similarity can be defined beyond these distances. Things are less clear for jets, but when looked at in detail, $\mathrm{d}A/\mathrm{d}z^*$ decreases by half between $z^* = 15$ ($\mathrm{d}A/\mathrm{d}z^* \approx 0.0075$) and $z^* = 65$ ($\mathrm{d}A/\mathrm{d}z^* \approx 0.0038$). The rate of evolution of A is thus not constant but decreases with z^* and tends to 0 at large z^*. These results provide support for a universal asymptotic regime with, however, different evolutions for jets and plumes.

4. Conclusions

George (1989) has postulated that differences in entrainment measured in different jet experiments were due to local self-similarity. A quantitative test of this idea

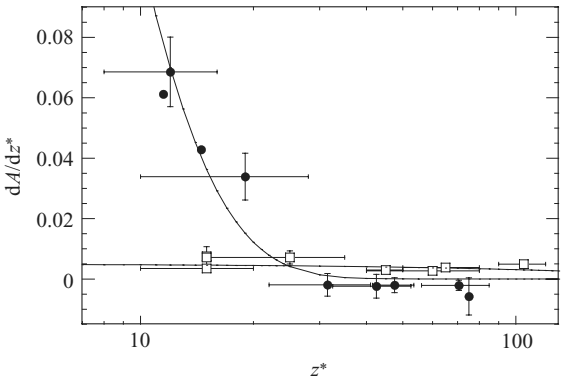

FIGURE 3. Rate of evolution of A in jets and plumes. The symbols the same as in figure 1. Solid lines are the derivatives of the consistent fits.

requires knowledge of the evolution of both the shapes of the profiles of dynamical variables and entrainment as a function of distance from the source. Most of the studies, however, have been carried out with ranges of z^* that are too small to provide a definitive test of the hypothesis of self-similarity. A global study of the different experiments shows however that the description based on local self-similarity proposed by George (1989) yields a better description of entrainment. Nevertheless, the global evolution of self-similarity follows a universal route, and complete self-similarity does eventually occur for both jets and plumes. According to Mi *et al.* (2001), non-identical states of self-similarity can be linked to the turbulence structures and in particular to more or less intermittent large-scale coherent structures. These structures are not present close to the source where the turbulence is still influenced by the geometry of the nozzle. At intermediate distances the large-scale structures appear but are only intermittent (Schefer *et al.* 1994). At large distances, they eventually become permanent and the flow is fully self-similar. These structures drive the evolution of the profiles and contribute to the changes of A.

The evolution of A can be due to the evolution of the shape of the profiles and/or to the evolution of the relative width of the buoyancy and velocity profiles which reflects the local turbulent Prandtl number. For example, taking $\lambda = 1$ one can analytically write A as a function of the power in the exponential expression for the velocity and buoyancy profiles, n,

$$A = 2^{4/n}3^{-2/n}. \tag{4.1}$$

Using that expression, one obtains that the evolution of the profiles from a 'top-hat' ($n \to \infty$) to a Gaussian shape ($n = 2$) increases the value of A from 1 to 1.33. This variation is significant but cannot account for the full range of observed values of A (table 2) which also requires a change of the turbulent Prandtl number. Figure 4 shows the values of λ and the corresponding values of the turbulent Prandtl number ($Pr = 1/\lambda^2$), which decrease from 1.61 to 0.83 in plumes and from 0.83 to 0.64 in jets. Such an evolution corresponds to the classical description in terms of momentum transport theory ($Pr \to 1$) close to the nozzle and in terms of vorticity transport theory ($Pr \to 0.5$) at large distances from the source (Schlichting 1955).

Our study shows that the route to self-similarity is different for jets and plumes. Not only does self-similarity occur earlier in pure plumes than in pure jets, but the

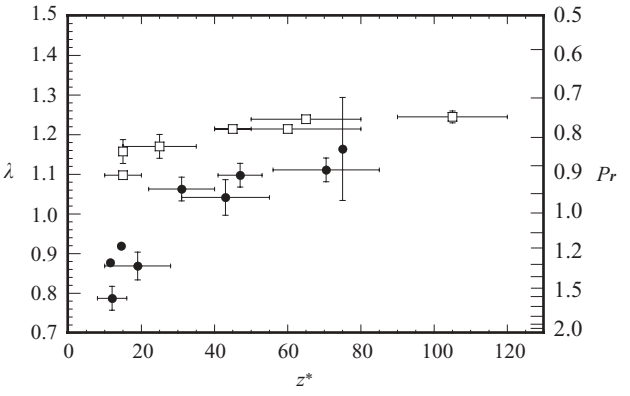

FIGURE 4. Evolution of λ (i.e. Pr) as a function of z^*. The symbols are the same as in figure 1.

effective turbulent Prandtl number is smaller in jets than in plumes. This suggests that buoyancy plays a role in triggering and organizing the large-scale structures, probably in relation to the buoyancy gradient between the core and the edges of a plume. As a result buoyancy has two important effects on entrainment: (i) directly via the term involving Ri in (2.1) and (ii) indirectly via the evolution of A in the term $\mathrm{d}A/\mathrm{d}z^*$ in (2.1). This emphasizes that additional care must be taken in experiments when it is intended to use passive tracers that generate some buoyancy.

The present study is based on the comparison of different studies made on different fluids, using different set-up and at different downstream distance from the source. We show that the evolution with downstream distance is the major effect. A clear understanding of the influence of other experimental parameters will in turn require the largest range possible of z^* in the measurements made in one given set of experiments and an explicit correction for the evolution of self-similarity. The quantitative description of a reference route to self-similarity in jets and plumes we provide may thus open the way to future experimental and theoretical work on the subject. For example, the more complex question of the transition between jet- and plume-like behaviour, for both lazy and forced plumes, could be revisited in the light of our new results.

The authors thank three anonymous referees for their constructive comments.

Appendix

Our approach is based on local measurement of the entrainment coefficient based on the shape of the velocity profile. An alternative approach is to estimate the entrainment coefficient from the measurement of the fluxes of mass and momentum. This approach requires in turn taking into account the finite fluxes of mass and momentum at the origin, which corresponds to the 'virtual origin' correction. This method has been applied successfully for lazy plumes (Hunt & Kaye 2001) and here we discuss its consequences for forced plumes.

In an unstratified environment and with the hypothesis of constant entrainment coefficient, the conservation equations can be written as (Morton *et al.* 1956;

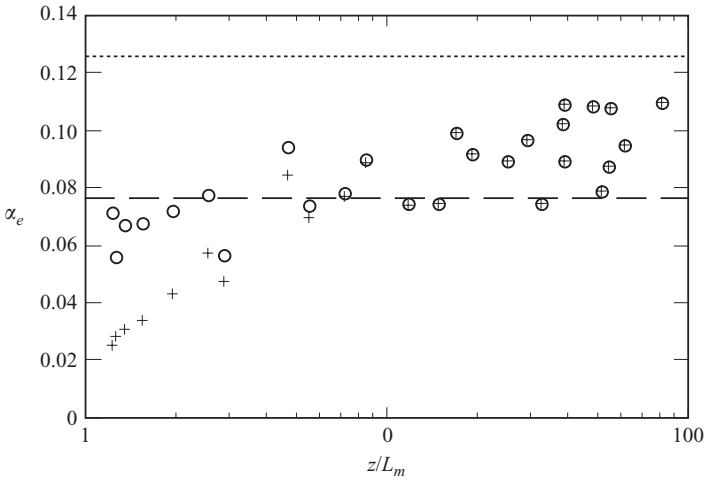

FIGURE 5. Evolution of α_e in jets and plumes obtained from the measurement of mass and momentum fluxes in Papanicolaou & List (1988). The open circles give the values corrected for the source fluxes whereas the crosses give the uncorrected values. The long-dashed line and dotted line give the local entrainment coefficient based on the profile of velocity in the pure-jet regime and in the pure-plume regime, respectively.

Linden 2000)

$$\frac{\mathrm{d}Q}{\mathrm{d}z} = 2\pi^{1/2}\alpha_e M^{1/2}, \tag{A 1}$$

$$\frac{\mathrm{d}M}{\mathrm{d}z} = \frac{QF}{M}, \tag{A 2}$$

$$\frac{\mathrm{d}F}{\mathrm{d}z} = 0, \tag{A 3}$$

where $Q = \pi w_m b^2$, $M = \frac{1}{2}\pi w_m^2 b^2$ and $F = \frac{1}{2}\pi g'_m w_m b^2$. Equations (A 1) and (A 2) can be combined to yield a value of α_e (Hunt & Kaye 2001),

$$\alpha_e = \frac{5F_0}{8\pi^{1/2}} \frac{Q^2 - Q_0^2}{M^{5/2} - M_0^{5/2}}, \tag{A 4}$$

where Q_0 and M_0 are fluxes at the source. The change in the entrainment coefficient corresponding to the source correction is then given as

$$\frac{\Delta\alpha_e}{\alpha_e} = \frac{1 - Q_0^2/Q^2}{1 - M_0^{5/2}/M^{5/2}} - 1. \tag{A 5}$$

Using (A 5) equation we found that the correction for the forced plumes considered in the present study is smaller than 1% and cannot account for the systematic change of α_e as a function of z/D on which we focus. This reflects the fact that measurements are made at large distances to the source relative to the mass length scale $L_a = Q^{3/5}/F^{1/5}$ which quantifies the distance over which the source volume flux is important (Fischer *et al.* 1979; Linden 2000).

In Papanicolaou & List (1988), the mass and momentum fluxes are given both at the origin and as a function of the downstream distance from the source, and equation (A 4) can be used to obtain a local value of the entrainment coefficient. Figure 5 shows the resulting evolution of α_e as a function of z/L_m, with and without

the correction of virtual origin. Three conclusions can be drawn from the figure. First, as noted before, the correction is negligible for $z/L_m > 5$, i.e. in the pure plume regime. Second, the entrainment coefficient is not constant but evolves as a function of z/L_m which is at odds with the underpinning hypothesis of the method. Last, the estimated entrainment coefficient is smaller than the one measured locally from velocity profiles, both for jets and for plumes. This is due to the fact that this method reflects the complete entrainment history of the plumes. In the pure-jet regime, the average entrainment appears reduced because of the stage of a potential core in which the profiles are not fully developed. In the pure-plume regime, the average entrainment appears reduced because of the stage of a pure jet in which buoyancy is not large enough to increase entrainment. One should note however that there is a systematic increase of the average entrainment towards the local pure-plume value. We thus conclude that although the method based on the virtual origin still shows an evolution of the entrainment coefficient, this evolution is biased by the past history of the plume, i.e. the fact that it started life as a jet. This method thus cannot be used as directly as the values obtained by measurement of local velocity profiles to study precisely the evolution of self similarity.

REFERENCES

Chen, J. C. & Rodi, W. (Eds.) 1980 *Turbulent Buoyant Jets – A Review of Experimental Data*. Pergamon.

Fischer, H. B., List, E. J., Koh, R. C. Y., Imberger, J. & Brooks, N. H. (Eds.) 1979 *Mixing in Inland and Coastal Waters*. Academic.

Forstall, W. & Gaylord, E. W. 1955 Momentum and mass transfer in a submerged water jet. *J. Appl. Mech.* **22**, 161–164.

George, W. K. 1989 The self-preservation of turbulent flows and its relation to initial conditions and coherent structures. In *Recent Advances in Turbulence* (ed. R. E. A. Arndt & W. K. George). Hemisphere.

George, W. K., Alpert, R. L. & Tamanini, F. 1977 Turbulence measurements in an axisymmetric buoyant plume. *Intl J. Heat Mass Transfer* **20**, 1145–1154.

Hunt, G. R. & Kaye, N. G. 2001 Virtual origin correction for lazy turbulent plumes. *J. Fluid Mech.* **435**, 377–396.

Kaminski, E., Tait, S. & Carazzo, G. 2005 Turbulent entrainment in jets with arbitrary buoyancy. *J. Fluid Mech.* **526**, 361–376.

Linden, P. F. 2000 Convection in the environment. In *Perspectives in Fluid Dynamics* (ed. G. K. Batchelor, H. K. Moffatt & M. G. Worster). Cambridge University Press.

List, E. J. 1982 Turbulent jets and plumes. *Annu. Rev. Fluid Mech.* **14**, 189–212.

Mi, J., Nobes, D. S. & Nathan, G. J. 2001 Influence of jet exit conditions on the passive scalar field of an axisymmetric free jet. *J. Fluid Mech.* **432**, 91–125.

Morton, B. R., Taylor, F. R. S. & Turner, J. S. 1956 Turbulent gravitationnal convection from maintained and instantaneous source. *Proc. R. Soc. Lond.* A **234**, 1–23.

Nakagome, H. & Hirita, M. 1977 The structure of turbulent diffusion in a axisymmetrical thermal plume. In *Proc. 1976 ICHMT Seminar on Turbulent Buoyant Convection*, pp. 361–372.

Panchapakesan, N. R. & Lumley, J. L. 1993 Turbulent measurements in axisymmetric jets of air and helium. Part 2. Helium jet. *J. Fluid Mech.* **246**, 225–247.

Papanicolaou, P. N. & List, E. J. 1988 Investigations of round vertical turbulent buoyant jets. *J. Fluid Mech.* **195**, 341–391.

Priestley, C. H. B. & Ball, F. K. 1955 Continuous convection from an isolated source of heat. *Q. J. R. Met. Soc.* **81**, 144–157.

Richards, C. D. & Pitts, W. M. 1993 Global density effects on the self-preservation behaviour of turbulent free jets. *J. Fluid Mech.* **254**, 417–435.

Rosensweig, R. E., Hottel, H. C. & Williams, G. D. 1961 Smoke-scattered light measurement of turbulent concentration fluctuations. *Chem. Engng Sci.* **15**, 111–129.

Rouse, H., Yih, C. S. & Humphreys, H. W. 1952 Gravitationnal convection from a boundary source. *Tellus* **4**, 201–210.

Ruden, P. 1933 Turbulente ausbreitungsvorgange im freistrahl. *Naturwissenschaft* **5**, 375–378.

Schefer, R. W., Kerstein, A. R., Namazian, M. & Kelly, J. 1994 Role of large-scale structure in a nonreacting turbulent CH_4 jet. *Phys. Fluids* **6**, 652–661.

Schlichting, H., ed. 1955 *Boundary-Layer Theory*. McGraw-Hill.

Schmidt, W. 1941 Turbulente ausbreitung eines stromes erhitzter luft. *Z. Angew. Math. Mech.* **21**, 351–363.

Shabbir, A. & George, W. K. 1994 Experiments on a round turbulent buoyant plume. *J. Fluid Mech.* **275**, 1–32.

Wang, H. & Law, A. W.-K. 2002 Second-order integral model for a round turbulent buoyant jet. *J. Fluid Mech.* **459**, 397–428.